Journal of Optoelectronics and Advanced Materials Vol. 7, No. 6, December 2005, p. 2985 - 2990

EFFECTS OF THERMAL TREATMENT ON THE LUMINESCENCE OF YAG:Eu NANOCRYSTALS SYNTHESIZED BY A NITRATE-CITRATE SOL-GEL METHOD

S. Georgescu*, A. M. Chinie, A. Stefan, O. Toma

National Institute for Laser, Plasma and Radiation Physics, Bucharest-Magurele, Romania

YAG:Eu nanopowders were synthesized by the nitrate-citrate sol-gel method. The morphologic modifications of the nanocrystallites produced by the thermal treatments at various temperatures are monitored by two parameters obtained from optical fluorescence spectroscopy: intensity ratio of the transition $^5D_0 \rightarrow {}^7F_2$ and $^5D_0 \rightarrow {}^7F_1$ and the maximum splitting of the $^7F_1$ level. An abrupt change of both parameters is observed at the amorphous-crystalline phase transition, followed by their gradual decrease with the annealing temperature. This fact was explained by an increase of the symmetry of the Eu^{3+} ion neighborhood.

(Received October 14, 2005; accepted November 24, 2005)

Keywords: YAG:Eu, Luminescence, Nanocrystal, Sol-Gel method

1. Introduction

Rare-earth-doped yttrium aluminum garnet (YAG) materials have wide applications as solid state laser media and are promising phosphor candidates [1-10]. Recently, high quality ceramic active media were obtained and characterized [11-14].

Powders of YAG doped with various rare earth ions can be obtained by the sol-gel route [6, 15-21]. In contrast with the solid state reaction which requires high temperatures (> 1600 °C) [22], the YAG phase is obtained by the sol-gel route at significantly lower temperatures (~ 900 °C), without any other parasitic phase.

Eu^{3+} -doped oxides are very efficient red phosphors. Extensive studies were devoted to Eu^{3+} -doped Y_2O_3 [23-31] but only few papers concerning the fluorescence properties of Eu^{3+}: YAG nanopowders were published [2-6, 21].

Besides the efficient luminescence, the peculiarities of the emission transitions make Eu^{3+} ion an ideal probe, very sensitive to any changes of its neighborhood.

In a previous paper [32] we reported on some preliminary results concerning the structural and spectroscopic properties of nanopowders of YAG doped with Er^{3+}, Eu^{3+}, and Tb^{3+} prepared by a nitrate-citrate sol-gel method and annealed at various temperatures between 600 and 1400 °C. Thus, the transition amorphous to crystalline phase took place in a relatively narrow temperature interval (900-930 °C) and the crystallites dimension increases with the annealing temperature. The phase transition was put in evidence using X-ray diffraction, FT-IR and fluorescence spectroscopy.

In this paper we continue the studies of the modifications induced in the nanopowders of YAG:Eu by the thermal treatment using the fluorescence spectroscopy. In this aim, we analyze the splitting of the luminescence lines and the changes of the transition probabilities.

2. Experimental

The YAG nanocrystals were obtained by a nitrate-citrate sol-gel method. Details can be found in [32].

* Corresponding author: joe@pluto.infim.ro

Thermal treatments were applied at successively increasing temperatures in the interval 600-1400 ºC. Optical measurements were performed on powder samples annealed at 900, 930, 1000, 1100, 1200, 1300, and 1400 ºC.

The luminescence of the YAG:Eu nanocrystals was excited at room temperature with a Xe lamp with suitable filters and gathered into a GDM 1000 monochromator equipped with an S-1 photomultiplier in the photon-counting configuration. The spectra were recorded using a TURBO MCS scaler. The pump takes place in a wavelength domain centered at 390 nm, spanning the transition $^7F_0 \rightarrow {}^5L_6$. The luminescence spectra were not corrected for the spectral sensitivity of the experimental set-up.

3. Results and discussion

Europium substitutes the Y^{3+} ion in the garnet lattice, entering the dodecahedral position with the local symmetry D_2, as Eu^{3+}. Part of the energy level scheme of Eu^{3+} (^7F_J, and $^5D_{J'}$ multiplets) is given in Fig. 1.

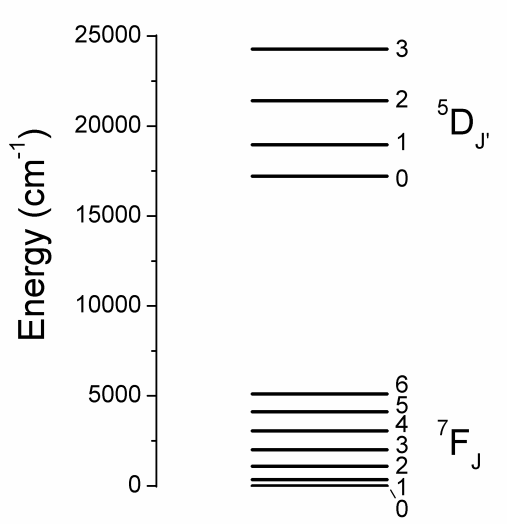

Fig. 1. Part of the energy level scheme of Eu^{3+}.

Due to the large phonons of YAG, only the fluorescence lines originating from $^5D_0$ are clearly observed in the fluorescence spectra. Therefore, we will discuss only the transitions $^5D_0 \rightarrow {}^7F_J$. A detailed discussion regarding the optical transitions in bulk YAG:Eu is given in [33].

In D_2 symmetry the transitions $\Gamma_i \leftrightarrow \Gamma_i$ are forbidden for both electric and magnetic dipole [34]. $^5D_0$ and $^7F_0$ transform in D_2 as Γ_1 (the totally symmetric representation). Therefore, the transition $^5D_0 \rightarrow {}^7F_0$ is forbidden in this symmetry. $^7F_1$ splits in three crystal field sublevels having the symmetry Γ_2, Γ_3 and Γ_4 respectively, all the three lines belonging to the magnetic dipole transition $^5D_0 \rightarrow {}^7F_1$ could be observed. In D_2 $^7F_2$ splits in five sublevels ($2\Gamma_1 + \Gamma_2 + \Gamma_3 + \Gamma_4$) but only three fluorescence lines belonging to the electric dipole transition $^5D_0 \rightarrow {}^7F_2$ could be observed (transitions $\Gamma_1 \leftrightarrow \Gamma_1$ are forbidden) and so on.

In the amorphous phase the local symmetry is lower and all the transitions are allowed. In Fig. 2 is shown the fluorescence spectrum for powder annealed at 900 °C in the spectral domain 11500 – 17500 cm^{-1}. This spectral domain spans the transitions $^5D_0 \rightarrow {}^7F_J$ (J = 0,…,6), marked F_J in Fig. 2. We note the presence of the fluorescence line corresponding to the transition $^5D_0 \rightarrow {}^7F_0$. The fluorescence lines are wide, characteristic for the amorphous phase.

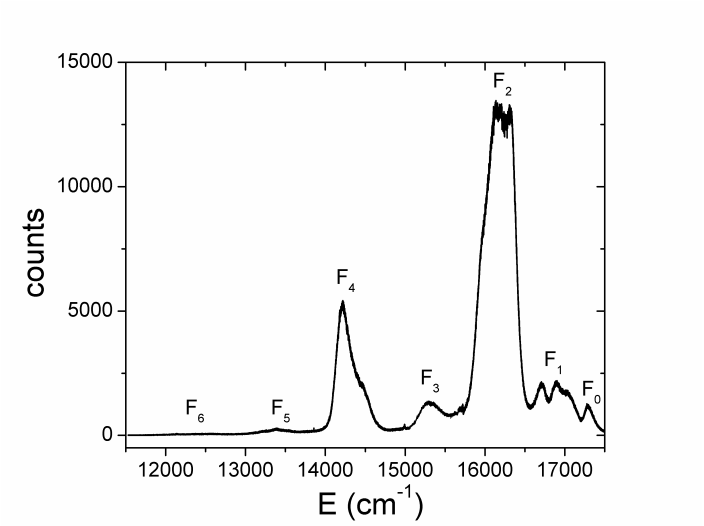

Fig. 2. The luminescence spectrum (transitions $^5D_0 \rightarrow {}^7F_J$, J = 0,…,6) of the powder annealed at 900 °C. The luminescence lines are wide, characteristic for the amorphous phase.

The fluorescence spectrum (in the same spectral domain) of the powder sample annealed at 930 °C is presented in Fig. 3. A drastic change of the luminescence spectrum is observed. This time the fluorescence lines are narrow, characteristic for the crystalline (garnet) phase. This means that in the temperature interval 900-930 °C takes place the transition amorphous – crystalline. This transition was confirmed by X-ray diffraction and FT-IR measurements [32]. Since now the symmetry at the Eu^{3+} position is D_2, the transition $^5D_0 \rightarrow {}^7F_0$ is no longer observed.

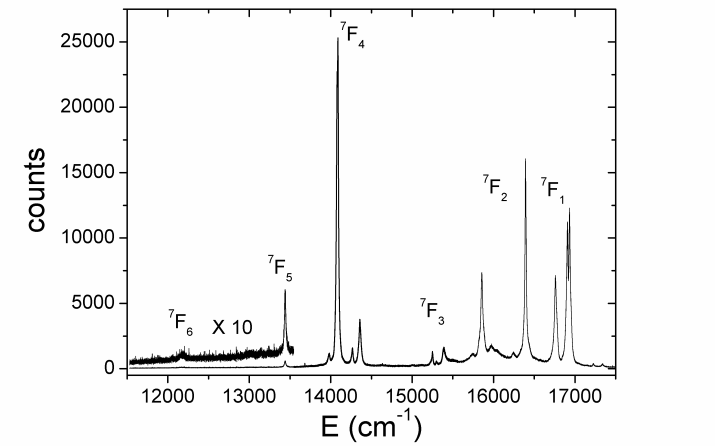

Fig. 3. The luminescence spectrum (transitions $^5D_0 \rightarrow {}^7F_J$, J = 0,…,6) of the powder annealed at 930 °C. This time, the luminescence lines are narrow, characteristic for the crystalline phase.

With annealing temperature increases the apparent average crystallite size for the YAG:Eu nanopowder [32]. In the annealing temperature interval 930-1300 °C, this size increases from 32 nm to 82 nm. Obviously, the optical properties of the YAG:Eu nanopowders depend on the crystallite properties (dimension and shape distribution) but is more convenient to represent the results function of the annealing temperature. In fact, the measured properties are the result of averaging in individual crystallites (function of the ratio / surface volume) and of the averaging on the crystallite size distribution in powder.

For higher annealing temperatures (larger crystallites) the fluorescence lines become narrower. The annealing temperature dependence of the linewidth for two well isolated lines of the transition $^5D_0 \rightarrow {}^7F_4$ was given in [32].

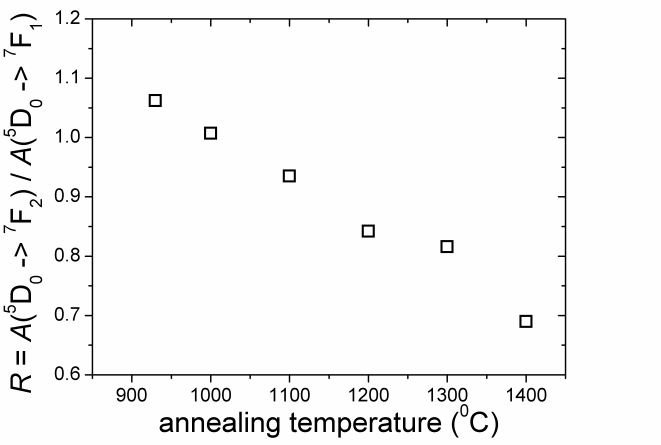

Fig. 4. The ratio of the areas of the electric dipole transition ($^5D_0 \rightarrow {}^7F_2$) and magnetic dipole transition ($^5D_0 \rightarrow {}^7F_1$) function of the annealing temperature of the YAG:Eu nanopowders.

The transition $^5D_0 \rightarrow {}^7F_1$ is a magnetic dipole one. The magnetic dipole transitions are parity allowed and their intensity is practically not sensitive at the changes in the neighborhood of the Eu^{3+} ion. On the other hand, the electric dipole transition $^5D_0 \rightarrow {}^7F_2$ (a hypersensitive transition [35, 36]) is very sensitive to the structural changes. Therefore, the usual practice [37] is to monitor the ratio of the transition intensities $R' = I(^5D_0 \rightarrow {}^7F_2) / I(^5D_0 \rightarrow {}^7F_1)$, the intensity of the magnetic dipole transition playing the role of an internal standard. Because the transition intensities are proportional with the area under the fluorescence lines, we shall calculate the ratio of the respective areas: $R = A(^5D_0 \rightarrow {}^7F_2) / A(^5D_0 \rightarrow {}^7F_1)$. The dependence of this ratio on the annealing temperature is presented in Fig. 4.

The ratio R decreases significantly with the annealing temperature (approximately 1.5 times) denoting an increase of the local symmetry [37]. The higher the symmetry, the lower is the ratio R. We note that for the amorphous powder (lower local symmetry- (Fig. 3)) this ratio is close to 7.

Another measurable indicator of the evolution of the nanocrystalline YAG:Eu powders with the annealing temperature is the maximum splitting of the $^7F_1$ level, ΔE [38, 39]. As we already discussed, all the three lines of the $^7F_1$ level are visible in the fluorescence spectrum.

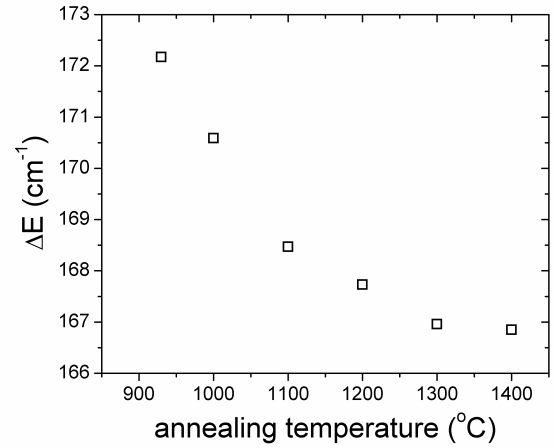

Fig. 5. Dependence of the maximum splitting of the $^7F_1$ level (ΔE) function of the annealing temperature.

In Fig. 5 we observe a reduction of the maximum splitting of the $^7F_1$ level with increasing annealing temperature from approx. 172 cm^{-1} to 167 cm^{-1}. We note that the value of 167 cm^{-1}, obtained for the YAG:Eu powder annealed at 1400 °C, corresponds to the bulk material value [40]. For the amorphous powder (annealed at 900 °C, Fig. 2) the maximum splitting is much larger: 328 cm^{-1}. Since the value of the maximum splitting is proportional with the crystal field intensity [38, 39], the intensity of the crystal field decreases with the increase of the annealing temperature, i.e. the crystal field intensity decreases with the increase of the crystallite dimension.

The ratio surface / volume decreases with the crystallite dimension. Therefore, we could link the observed effects (the reduction of the ratio of the transition intensities $R' = I(^5D_0 \rightarrow {}^7F_2) / I(^5D_0 \rightarrow {}^7F_1)$ and the decrease of the maximum splitting of $^7F_1$ level, i.e. the reduction of the crystal filed intensity) with the reduction of the relative influence of the surface of the nanocrystals. The Eu^{3+} ions in sites close to the surface "see" a modified crystal field in rapport with the Eu^{3+} ions placed inside the nanocrystal. The near surface sites have a lower symmetry. Though the monitored parameters evidence an increase of Eu^{3+} neighborhood symmetry with the annealing temperature, the symmetry of the neighborhood in the nanocrystals immediately after the phase transition is close to D_2. This fact is evidenced by the absence of transition $^5D_0 \rightarrow {}^7F_0$ in the fluorescence spectrum of the nanocrystals immediately after the phase transition.

4. Conclusions

In this paper we used the optical fluorescence spectroscopy to monitor the evolution of the YAG:Eu nanocrystals with annealing temperature. Thus, the fluorescence spectrum exhibits a drastic change at the amorphous-crystalline phase transition (narrow fluorescence lines instead of large ones, the line corresponding to the $^5D_0 \rightarrow {}^7F_0$ disappears). Increasing the annealing temperature, the intensity ratio of the transitions $^5D_0 \rightarrow {}^7F_2$ (electric dipole) and $^5D_0 \rightarrow {}^7F_1$ (magnetic dipole) and the maximum splitting of the $^7F_1$ level decrease denoting an increase of the local symmetry and a reduction of the crystal field intensity at the Eu^{3+} position. Both aspects could be related to the reduction of the influence of the surface of the nanocrystals with the increase of the crystallite dimensions.

Acknowledgments

This work was supported by the CERES Project C4-199/2004.

References

[1] A. A. Kaminskii, Laser crystals: their physics and properties, 2-nd edition, Springer series in optical sciences, vol. 14, (Springer, Berlin, 1990).
[2] S. Shikao, W. Jiye, J. Alloys Compounds **327**, 82 (2001).
[3] Y. H. Zhou, J. Lin, M. Yu, S. M. Han, S. B. Wang, H. J. Zhang, Mat. Res. Bull. **38**, 1289 (2003).
[4] J. J. Zhang, J. W. Ning, X. J. Liu, Y. B. Pan, L. P. Huang, J. Mat. Sci. Lett. **22**, 13 (2003)
[5] C. H. Lu, W. T. Hsu, J. Dhanaraj, R. Jagannathan, J. Eur. Cer. Soc. **24**, 3723 (2004).
[6] G. Xia, S. Zhou, J. Zhang, S. Wang, Y. Liu, J. Xu, J. Crystal Growth **283**, 257 (2005).
[7] Y. Hakuta, K. Seino, H. Ura, T. Adschiri, H. Takizawa, K. Arai, J. Mat. Chem. **9**, 2671 (1999).
[8] X. Li, H. Liu, J. Wang, H. Cui, S. Yang, I. R. Boughton, J. Phys. Chem. Solids **66**, 201 (2005).
[9] Y. Zhou, J. Lin, M. Yu, S. Wang, H. Zhang, Mat. Lett. **56**, 628 (2002).
[10] Y. Pan, M. Wu, Q. Su, Mat. Sci. Eng. B **106**, 251 (2004).
[11] A. Ikesue, T. Kinoshita, K. Kamata, K. Yoshida, J. Am. Ceram. Soc. **78**, 1033 (1995).
[12] A. Ikesue, K. Yoshida, T. Yamamoto, I. Yamaga, J. Am. Ceram. Soc. **80**, 1517 (1997).
[13] V. Lupei, A. Lupei, S. Georgescu, T. Taira, Y. Sato, A. Ikesue, Phys. Rev. B **64**, 092102 (2001).

[14] V. Lupei, A. Lupei, S. Georgescu, B. Diaconescu, T. Taira, Y. Sato, S. Kurimura, A. Ikesue, J. Opt. Soc. Am. B **19**, 360 (2002).
[15] B. J. Chung, J. Y. Park, S. M. Sim, J. Ceram. Proc. Res. **4**, 145 (2003).
[16] M. Veith, S. Mathur, A. Kareiva, M. Jilavi, M. Zimmer, V. Huch, J. Mater. Chem., **9**, 3069 (1999).
[17] Q. Lu, W. Dong, H. Wang, X. Wang, J. Am. Ceram. Soc. **85**, 490 (2002).
[18] D. Hreniak, W. Strek, J. Alloys Compounds **341**, 183 (2002).
[19] I. Muliuoliene, S. Mathur, D. Jasaitis, H. Shen, V. Sivakov, R. Rapalaviciute, A. Beganskiene, A. Kareiva, Opt. Mat. **22**, 241 (2003).
[20] D. Hreniak, W. Strek, P. Mazur, R. Pazik, M. Zazbkowska-Wacławek, Optical Materials **26**, 117 (2004).
[21] D. Boyer, G. Bertrand-Chadeyron, R. Mahiou, Opt. Mat. **26**, 101 (2004).
[22] A. Ikesue, K. Kamata, K. Yoshida, J. Am. Ceram. Soc. **78**, 2545 (1995).
[23] E. P. Reidel, J. Lumin. **1-2**, 176 (1970).
[24] K. S. Hong, R. S. Meltzer, B. Bihari, D. K. Williams, B. M. Tissue, J. Lumin. **76-77**, 234 (1998).
[25] A. Konrad, T. Fries, A. Gahn, F. Kummer, U. Herr, R. Tidecks, K. Samwer, J. Appl. Phys. **86**, 3129 (1999).
[26] T. Igarashi, M. Ihara, T. Kusunoki, K. Ohno, T. Isobe, M. Senna, Appl. Phys. Lett. **76**, 1549 (2000).
[27] G. Wakefield, E. Holland, P. J. Dobson, J. L. Hutchison, Adv. Mater. **13**, 1557 (2001).
[28] D. R. Tallant, C. H. Seager, R. L. Simpson, J. Appl. Phys. **91**, 4053 (2002).
[29] K. Zhang, A. K. Pradhan, G. B. Loutts, U. N. Roy, Y. Cui, A. Burger, J. Opt. Soc. Am. B **21**, 1804 (2004).
[30] N. Joffin, J. Dexpert-Ghys, M. Verelst, G. Baret, A. Garcia, J. Lumin. **113**, 249 (2005).
[31] M. V. Nazarov, J. H. Kang, D. Y. Jeon, E. -J. Popovici, L. Muresan, B. S. Tsukerblat, Solid State Communications **133**, 183 (2005).
[32] A. M. Chinie, A. Stefan, S. Georgescu, O. Toma, E. Borca, M. Bercu, presented at the 6th International Balkan Workshop on Applied Physics, July 5-7th, 2005, Constanta, Romania, to be published in J. Optoelectron. Adv. Mater. **8**(1), 2006.
[33] H. Gross, J. Neukum, J. Heber, D. Mateika, T. Xiao, Phys. Rev. B **48**, 9264 (1993).
[34] G. F. Koster, J. O. Dimmock, R. G. Wheeler, H. Statz, Properties of the thirty-two point groups, MIT Press, Cambridge, Massachusetts, 1963.
[35] C. K. Jørgensen, B. R. Judd, Mol. Phys. **8**, 281 (1964).
[36] R. D. Peacock, Structure and Bonding **22**, 83 (1975).
[37] R. Reisfeld, E. Zigansky, M. Gaft, Mol. Phys. **102**, 1319 (2004).
[38] F. Auzel, O. L. Malta, J. Physique **44**, 201 (1983).
[39] O. L. Malta, E. Antic-Fidancev, M. Lemaitre-Blaise, A. Milicic-Tang, M. Taibi, J. Alloys Comp. **283**, 41 (1995).
[40] Y. R. Shen, C. M. Li, V. C. Costa, K. L. Bray, Phys. Rev. B **68**, 014101 (2003).